Since January 2020 Elsevier has created a COVID-19 resource centre with free information in English and Mandarin on the novel coronavirus COVID-19. The COVID-19 resource centre is hosted on Elsevier Connect, the company's public news and information website.

Journal of Molecular Structure 1230 (2021) 129649

Contents lists available at ScienceDirect

Journal of Molecular Structure

journal homepage: www.elsevier.com/locate/molstr

Synthesis of potentially new schiff bases of *N*-substituted-2-quinolonylacetohydrazides as anti-COVID-19 agents

Mohammed B. Alshammari[a,*], Mohamed Ramadan[b], Ashraf A. Aly[c,**], Essmat M. El-Sheref[c], Md Afroz Bakht[a], Mahmoud A.A. Ibrahim[c], Ahmed M. Shawky[d]

[a] Chemistry Department, College of Sciences and Humanities, Prince Sattam bin Abdulaziz University, P.O. Box 83, Al-Kharij 11942, Saudi Arabia
[b] Department of Organic Pharmacy, Faculty of Pharmacy, Al-Azhar University, Assiut Branch, Egypt
[c] Chemistry Department, Faculty of Science, Minia University, El-Minia 61519, Egypt
[d] Science and Technology Unit (STU), Umm Al-Qura University, Makkah 21955, Saudi Arabia

ARTICLE INFO

Article history:
Received 15 May 2020
Revised 7 November 2020
Accepted 11 November 2020
Available online 16 November 2020

Keywords:
Quinolone
N-substituted-2-quinolonylacetohydrazides
Nmr
Remdesivir
Molecular docking

ABSTRACT

We report herein a new series of synthesized *N*-substituted-2-quinolonylacetohydrazides aiming to evaluate their activity towards SARS-CoV-2. The structures of the obtained products were fully confirmed by NMR, mass, IR spectra and elemental analysis as well. Molecular docking calculations showed that most of the tested compounds possessed good binding affinity to the SARS-CoV-2 main protease (M^{pro}) comparable to **Remdesivir**.

1. Introduction

Recently, human coronaviruses have attracted much interest. A new strain for Corona viruses (CoVs) identified in late December 2019 named SARS-CoV-2 resulted in a massive outbreak initially in Wuhan, China and propagated to different nations around the globe. The World Health Organization (WHO) declared the resulting disease named COVID-19 as a pandemic [1,2]. It is safe to say that a sufficient understanding of SARS-CoV-2, and the full clinical picture of the resulting COVID-19 disease will take some time [3-8].

Remdesivir (Fig. 1) an adenosine analogue, has been recently recognized as a promising antiviral drug against a wide array of RNA viruses (including SARS/MERS-CoV) [9,10] infection in cultured cells, mice and nonhuman primate (NHP) models. It is currently under clinical development for the treatment of the Ebola virus infection [11]. **Remdesivir** binds to ribonucleic acid (RNA)-dependent RNA polymerase and acts as an RNA-chain terminator. It displays potent *in vitro* activity against SARS-CoV-2 with an EC_{50} at 48 h of 0.77 μM in Vero E6 cells. **Remdesivir** is highly selective for viral polymerases and is therefore expected to have a low propensity to cause human toxicity [12].

During last few decades, 4–hydroxy-2-quinolones as privileged structures in drug discovery are beyond doubt, one of the major areas in medicinal chemistry [13-15]. The 4–hydroxy-2-quinolinones scaffold is widely found in alkaloids [16] and they are important as a characteristic building block for a series of significant biologically active compounds. Many efforts have been done on antiviral properties of quinolines and quinolones and their structural analogues against the human immunodeficiency virus (HIV), but their antiviral activity was also demonstrated against the human cytomegalovirus (HCMV), SARS corona virus, Zika virus, Chikungunya virus, hepatitis C virus (HCV), and Ebola virus [17-22]. The mechanism of action of antiviral quinolone remains unclear. Specific studies aimed at understanding the nature of drug's targets at the molecular level indicated that quinolones inhibit viral transcription [23].

Elvitegravir, (Fig. 2) is the first quinolone-based anti-HIV drug, exhibiting potent inhibitory activity against integrase-catalyzed DNA strand transfer [24,25]. Another series of quinolone-3-carboxylic acids have been synthesized by introducing different hydrophobic groups at the N(1), C(2), C(7), and C(8) positions [26]. Most of the compounds of this group showed anti-HIV activity without cytotoxicity at a concentration of 100 μM.

* Co-Corresponding author.
** Corresponding author.
E-mail addresses: m.alshammari@psau.edu.sa (M.B. Alshammari), ashrafaly63@yahoo.com (A.A. Aly).

https://doi.org/10.1016/j.molstruc.2020.129649
0022-2860/

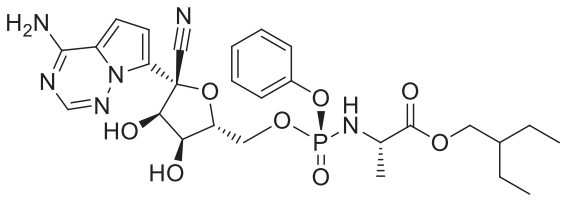

Fig. 1. Structure of Remdesivir.

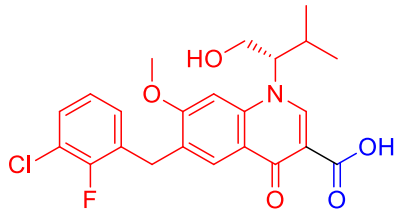

Fig. 2. Chemical structure of **Elvitegravir**.

Fig. 3 summarizes the work of Aly et al. in the synthesis of 4–hydroxy-2-quinolones of potential biologically active compounds. As an example, 2,3-bis-(4–hydroxy-2-oxo-1,2-dihydroquinolin-3-yl)succinic acid derivative **I**, was obtained by a one-pot reaction of one equivalent of aromatic amines with two equivalents of diethyl malonate in diphenyl ether and catalyzed with triethylamine [27]. A reaction of four equivalents of 4-hydroxyquinolin-2(1*H*)-one with one equivalent of acenaphthoquinone gave acenaphthylene-1,1,2,2-tetrayl-tetrakis(4-hydroxyquinolin-2(1*H*)-one) (**II**, [28]. We also reported that quinoline-2,4–dione reacted with 2-(2-oxo-1,2-dihydroindol-3-ylidene)malononitrile in pyridine to give spiro(indoline-3,4′-pyrano[3,2-*c*]quinoline)−3′-carbonitrile (**III**, [29], whereas 2-quinolone reacted with diethyl acetylenedicarboxylate to give pyrano[3,2-*c*]quinoline-4-carboxylate (**IV**, [30]. Also a class of 1,2,3-triazoles derived by 2-quinolone (**V**, [31]) was synthesized, *via* Cu-catalyzed [3 + 2]cycloadditions (Meldal-Sharpless 'click'-reactions) [31]. We also synthesized naphthofuro[3,2-*c*]quinoline-6,7,12-trione **VI**, and pyrano[3,2-*c*]quinoline-6,7,8,13-tetraone, **VII** that have shown potential as ERK inhibitors [32], whereas synthesis of bis(6-substituted-4–hydroxy-2-oxo-1,2-dihydroquinolin-3-yl)naphtha-ene-1,4–dione **VIII** and (substituted *N*-(alkyl)bis-quinolinone)-triethylammonium salt **VIV** [33], were explored as candidates for extracellular signal-regulated kinases 1/2 (ERK1/2) having antineoplastic activity [33]. Recently, we have reported the synthesis of 5,12-dihydro-pyrazino[2,3-*c*:5,6-*c'*]difuro[2,3-*c*:4,5-*c'*]-diquinoline-6,14(5H,12*H*)–dione **X** [34] and 2-(4–hydroxy-2-oxo-1,2-dihydroquinolin-3-yl)−1,4-diphenyl-butane-1,4–dione XI [34]. Most indicative is our recent synthesis of 6-substiuted-4-(2-(4-substituted-benzylidene)hydrazinyl)quinolin-2(1*H*)-one derivative **XII** [35] which was evaluated for their *in vitro* cytotoxic activity against 60 cancer cell lines according to NCI protocol [35].

On the other hand, Schiff bases have large importance in medicinal and pharmaceutical fields due to a broad spectrum of biological activities like analgesic [36–39], anti-inflammatory [36,38,40], anti-tubercular [41], anti-cancer [42,43], and so forth. So, from the highly biological and pharmaceutical activities of 4–hydroxy-2-quinolinones and Schiff bases, we focused in our paper to merging the activity of these compounds and compare them with **Remdesivir** (as one of the prospective drugs) against COVID-19.

2. Results and discussion

2.1. Chemistry section

Our research plane started by preparation of compounds **2a,b** during reaction between quinolones **1a,b** and ethyl bromoacetate. Compounds **2a,b** reacted with hydrazine in EtOH and gave the corresponding 2-((2-oxo-1,2-dihydroquinolin-4-yl)oxy)acetohydrazide **3a,b** in good yields (Scheme 1) [44,45]. By refluxing equimolar amounts of compounds **3a,b** with an aldehydes in absolute ethanol with few drops of acetic acid gave our target new Schiff bases **4a-k** in 75–90% yields (Scheme 1). The structure assignments of compounds **4a-k** were established using different spectroscopic tools like IR, NMR (^{1}H, ^{13}C, ^{15}N, 2D), elemental analyses and mass spectrometry. The elemental analysis showed that the corresponding molecular formula for all new compounds **4a-k** are formed form one molecule of compound **3a,b** and one molecule of the entered aldehyde with elimination

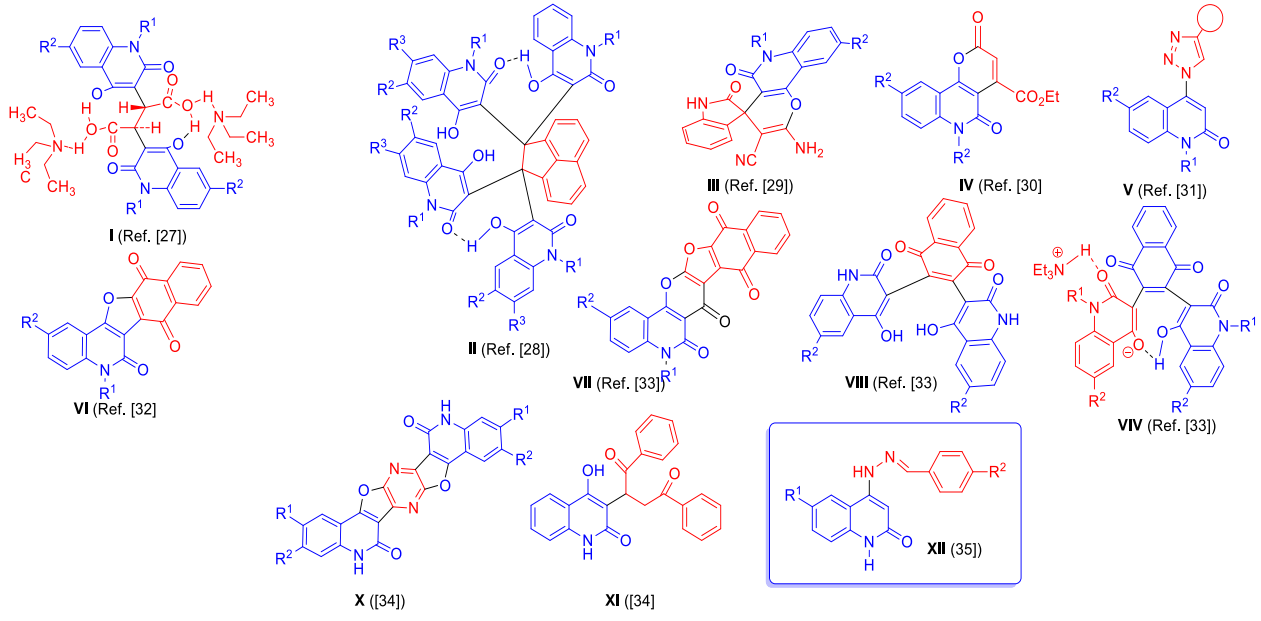

Fig. 3. Structures of compounds that previously reported 2-quinolones **I-XII**.

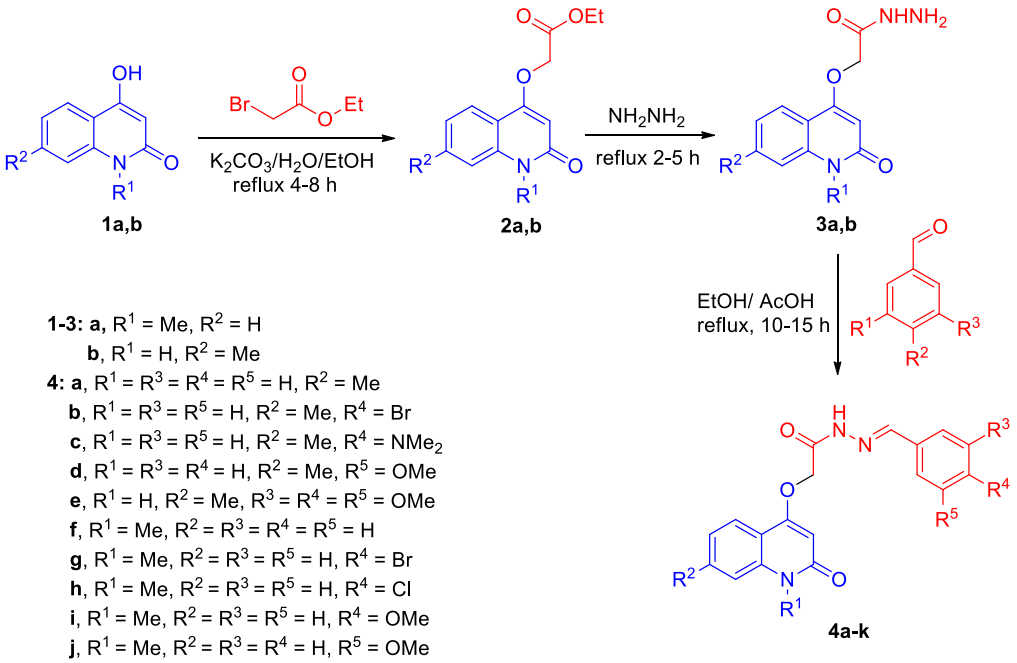

1-3: a, R^1 = Me, R^2 = H
b, R^1 = H, R^2 = Me
4: a, $R^1 = R^3 = R^4 = R^5$ = H, R^2 = Me
b, $R^1 = R^3 = R^5$ = H, R^2 = Me, R^4 = Br
c, $R^1 = R^3 = R^5$ = H, R^2 = Me, R^4 = NMe_2
d, $R^1 = R^3 = R^4$ = H, R^2 = Me, R^5 = OMe
e, R^1 = H, R^2 = Me, $R^3 = R^4 = R^5$ = OMe
f, R^1 = Me, $R^2 = R^3 = R^4 = R^5$ = H
g, R^1 = Me, $R^2 = R^3 = R^5$ = H, R^4 = Br
h, R^1 = Me, $R^2 = R^3 = R^5$ = H, R^4 = Cl
i, R^1 = Me, $R^2 = R^3 = R^5$ = H, R^4 = OMe
j, R^1 = Me, $R^2 = R^3 = R^4$ = H, R^5 = OMe
k, R^1 = Me, R^2 = H, $R^3 = R^4 = R^5$ = OMe

Scheme 1. Preparation of new Schiff bases **4a-k**.

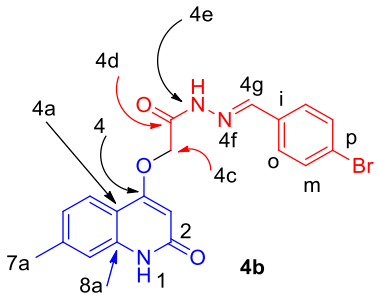

Fig. 4. (*E*)-*N*′-(4-Bromobenzylidene)−2-((7-methyl-2-oxo-1,2-dihydroquinolin-4-yl)oxy)-acetohydrazide (**4b**).

for a H_2O molecule. To illustrate the structure for the obtained compounds **4a-k**, we choose compound **4b** as an example which was assigned as *N*′-(4-bromobenzylidene)−2-((7-methyl-2-oxo-1,2-dihydroquinolin-4-yl)oxy)acetohydrazide (**4b**) with a molecular formula $C_{19}H_{16}BrN_3O_3$ (m/z = 414). Its IR spectrum did not show any absorption band corresponding to hydrazine-NH_2, thus indicated that condensation has occurred (Fig. 4).

This was fully supported by its ^{1}H NMR spectrum, which displayed a characteristic singlet at δ_H = 11.80, 11.34 ppm, integrating for two D_2O exchangeable protons which were assigned as NH-4e and NH-1, respectively. Also, a singlet at δ_H = 5.33 ppm (2H) corresponding to –OCH_2- (H-4c) was further confirmed from ^{13}C NMR (Fig. 5) with a characteristic singlet at δ_C = 65.15 ppm (Table 1).

The protons of the phenyl group exhibit a 1,4-disubstituted system and was observed as a double-doublet at δ_H = 7.72 (d, J = 8.5 Hz; 2H, H-o) and δ_H = 7.65 (d, J = 8.5 Hz; 2H, H-m) and both of them give a ^{1}H–^{1}H-COXY with each other (Table 1). The ^{13}C NMR spectrum for compound **4b** showed characteristic singlets at δ_C = 167.78, 163.25, 162.05, 147 and 21.28 which were assigned as C-4d, quinolone-C-2, C-4, *C* = *N* (C-4 g), and methyl group (C-7a), respectively (Table 2). In ^{15}N-NMR, the signal at δ_N = 317.2 ppm, indicated as N-4f gave HMBC correlation with

Table 1
^{1}H NMR for compound **4b**.

^{1}H NMR	^{1}H–^{1}H COSY	Assignment:
11.80 (s, 1H)		NH-4e
11.34 (s, 1H)	5.73	NH-1
8.01 (s, 1H)		H-4 g
7.76 (d, J = 8.2 Hz, 1H)	7.03	H-5
7.72 (d, J = 8.5 Hz, 2H)	7.65	H-o
7.65 (d, J = 8.5 Hz, 2H)	7.72	H-m
7.09 (s; 1H)	2.38	H-8
7.03 (d, J = 8.4 Hz; 1H)	7.81, 7.76	H-6
5.74 (s, 1H)	11.34	H-3
5.33 (s, 2H)		H-4c
2.38 (s; 3H)	7.09	H-7a

Table 2
^{13}C and ^{15}N NMR spectral data for compound **4b**.

^{13}C NMR	HSQC	HMBC	Assignment:
167.78		11.80, 11.79, 5.33, 5.30	C-4d
163.25		11.78, 5.33, 4.81, 2.89, 2.735	C-2
162.05		11.78, 7.76, 5.74, 5.33, 4.85, 2.89, 2.735	C-4
142.93	8.02, 8.01, 7.96	11.80, 11.79, 7.72	C-4 g
141.07		7.81, 7.76, 7.72	C-7
140.15		7.81, 7.76, 7.36	C-8a
133.20		8.29, 8.25, 8.02, 8.01, 7.65	C-*i*
131.74	7.67	7.67	C-*m*
129.02	7.72	7.65	C-*o*
123.20	7.03	7.72, 7.65, 7.09	C-*p*
122.76	7.81	7.09, 2.38	C-6
122.35	7.76	7.09, 2.38	C-5
114.88	7.09	11.34, 7.04, 6.95, 2.38	C-8
112.38		7.09, 5.74	C-4a
96.68	5.77, 5.74	11.34	C-3
65.15	5.33, 5.30, 4.85, 4.81	11.79	C-4c
21.28	2.38	7.09, 7.03	C-7a
^{15}N NMR	HSQC	HMBC	Assignment:
317.2		8.02, 8.01	N-4f
177.9	11.80, 11.79	8.02, 8.01	N-4e
144.4	11.39, 11.34		N-1

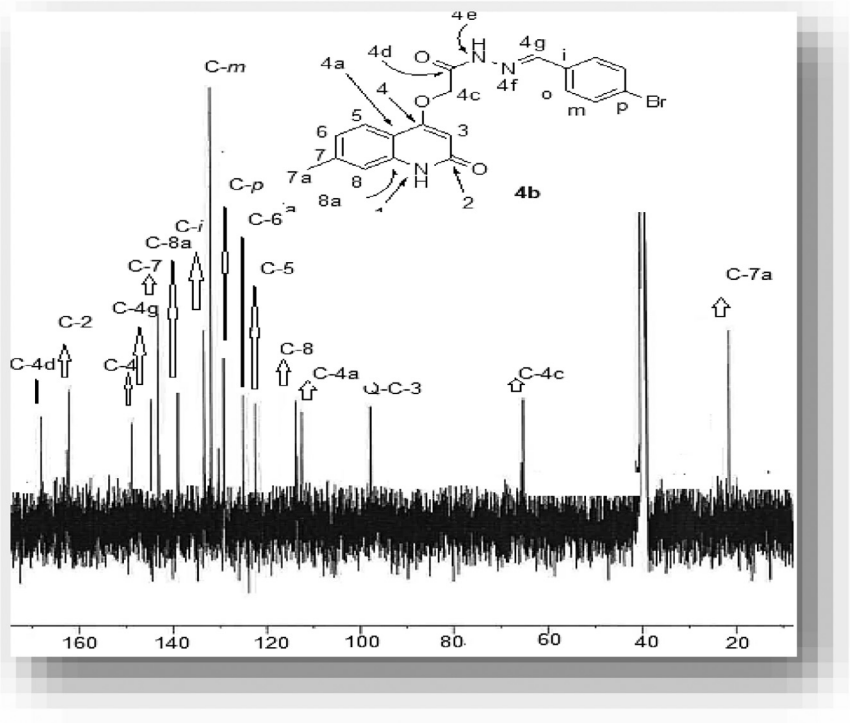

Fig. 5. ^{13}C NMR spectrum of **4b**.

proton at δ_H = 8.01 ppm which was assigned as H-4 g and didn't have any HSQC correlation, and this proton give HSQC correlation with carbon at δ_C = 142.93 ppm, which was assigned as C-4 g that indicates the absence of hydrazine-NH_2 and condensation takes place on it, with other signals at δ_N = 177.9 and 144.4 ppm, which were assigned as N-4e and N-1, respectively, and these nitrogen gave an HSQC correlation which indicates that these nitrogen atoms are carrying protons (Table 2). The former correlation indicates the *E*-form of the azomethine structure.

2.2. Molecular docking calculations

To reveal the binding modes and affinities of the synthesized compounds **4a-k** with SARS-CoV-2 main protease (M^{pro}) and RNA-dependent RNA polymerase (RdRp), molecular docking calculations were performed using Autodock4.2.6 software. The predicted docking scores and binding features of compounds **4a-k** with M^{pro} and RdRp receptors are listed in Table 3.

According to the calculated docking scores (Table 3), compounds **4a-k** showed good binding affinities towards M^{pro} with values in range −7.5 to −9.7 kcal/mol. Compared to main protease (M^{pro}), the synthesized compounds showed lower binding affinities towards RdRP with docking scores in range −6.5 to −7.7 kcal/mol. However, molecular docking of **Remdesivir** gave binding affinities of −8.5 and −5.6 kcal/mol with M^{pro} and RdRp, respectively (Table 3). Comparison of the binding affinities revealed that compound **4d** exhibited the largest binding affinities towards both of M^{pro} and RdRp with values of −9.7 and −7.7 kcal/mol, respectively. The high binding affinity of compound **4d** towards M^{pro} may be attributed to its potentiality to form four essential hydrogen bonds with lengths of 2.02, 2.22, 1.83 and 2.07 Å with LEU141, SER144, HIS163 and GLU166 amino acids, respectively (Fig. 6).

Analysis of the docked **4d**-RdRp complex, compound **4d** forms three essential hydrogen bonds with TYR619, ASP623 and GLU811 amino acids with average bond lengths of 2.19, 2.12 and 2.24 Å, respectively (Fig. 6). 2D LigPlus representations of interactions of

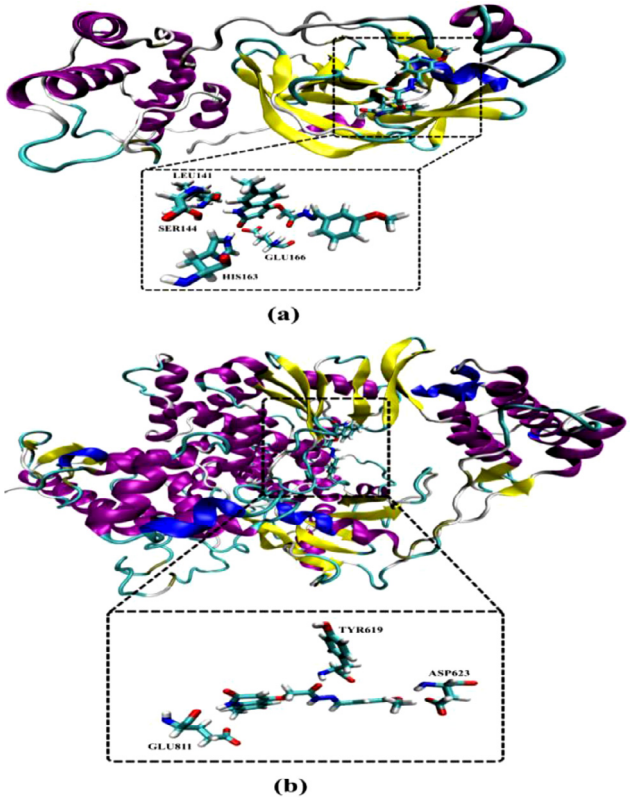

Fig. 6. Cartoon backbone representation of predicted binding modes of compound **4d** with SARS-CoV-2 (a) main protease (M^{pro}) and (b) RNA-dependent RNA Polymerase (RdRp). (For interpretation of the references to colour in this figure legend, the reader is referred to the web version of this article.)

Table 3
Calculated docking scores (in kcal/mol) and predicted binding features for compounds 4a-k with SARS-CoV-2 main protease (M^{pro}) and RNA-dependent RNA Polymerase (RdRp).

Compound	Main Protease (M^{pro})		RNA-dependent RNA Polymerase (RdRp)	
	Docking Score (kcal/mol)	Binding Features (Hydrogen bond length in Å)	Docking Score (kcal/mol)	Binding Features (Hydrogen bond length in Å)
4a	−9.1	GLU166 (1.89 Å), LEU141 (1.97 Å), HIS163 (1.97), SER144 (2.31 Å)	−7.3	TYR619 (2.15 Å), GLU811 (2.15 Å)
4b	−9.0	GLU166 (2.15 Å), SER144 (2.24 Å), LEU141 (1.99 Å)	−7.4	GLU811 (1.92 Å), TYR619 (2.07 Å)
4c	−7.7	ARG188 (1.82 Å), GLU166 (2.13 Å), MET165 (2.52 Å)	−7.5	TRP800 (1.91 Å), SER814 (1.92 Å)
4d	−9.7	SER144 (2.22 Å), GLU166 (2.07 Å), LEU141 (2.02 Å), HIS163 (1.83 Å)	−7.7	ASP623 (2.12 Å), TYR619 (2.19 Å), GLU811 (2.24 Å)
4e	−7.5	GLU166 (2.13 Å)	−7.3	TYR619 (2.08 Å), ASP623 (2.28 Å)
4f	−7.9	GLN189 (2.23 Å), GLY143 (1.75 Å)	−6.5	TYR619 (1.96 Å), TRP800 (1.96 Å)
4g	−8.2	GLU166 (2.32 Å), GLN192 (1.92 Å)	−7.6	ASP761 (1.69 Å), TRP800 (1.81 Å), SER814 (1.91 Å)
4h	−8.5	GLU166 (1.86 Å), GLN192 (1.99 Å)	−7.5	SER814 (1.97 Å), ASP761 (1.62 Å), TRP800 (1.96 Å)
4i	−8.6	GLU166 (1.86 Å), GLN192 (2.24 Å), SER144 (2.21 Å), CYS145 (2.37 Å)	−7.2	ASP761 (1.68 Å), TRP800 (1.78 Å), SER814 (1.86 Å)
4j	−8.7	GLU166 (2.21 Å), GLN192 (2.19 Å)	−7.5	TRP800 (1.90 Å), ASP760 (2.06 Å), LYS621(1.94 Å)
4k	−8.8	GLU166 (2.02 Å), HIS163 (1.93 Å), GLN192 (2.22 Å)	−7.6	TYR619 (2.78 Å), TRP800 (1.78 Å), ASP623 (2.02 Å), LYS621 (1.88 Å)

compounds **4a-k** with important amino acid residues of SARS-CoV-2 M^{pro} are depicted in Fig. 7. Overall, the molecular docking results could support the postulation that the synthesized compounds may act as potent SARS-CoV-2 M^{pro} inhibitors.

3. Conclusion

In conclusion, a new series of *N*-substituted-2-quinolonylacetohydrazides was here synthesized in order to evaluate their activity towards SARS-CoV-2 M^{pro} and RdRp. The NMR spectra (^{1}H, ^{13}C, ^{15}N, 2D) were used to prove the structure of the isolated compounds. Molecular docking calculations showed that most of the tested compounds possessed good binding affinity to the main protease (M^{pro}) comparable to **Remdesivir**. Analysis of the docked (*E*)-*N*'-(3-methoxybenzylidene)−2-((7-methyl-2-oxo-1,2-dihydroquinolin-4-yl)oxy)acetohydrazide-RdRp complex shows formation of three essential hydrogen bonds with TYR619, ASP623 and GLU811 amino acids with average bond lengths of 2.19, 2.12 and 2.24 Å, respectively. Much work has be done to evaluate more quinolones compounds, especially in the direction to find out how drugs capable to treat infections caused by the SARS-CoV-2 virus.

4. Experimental

Melting points were determined on Stuart electrothermal melting point apparatus and were uncorrected. TLC analysis was performed on analytical Merck 9385 silica aluminum sheets (Kiselgel 60) with PF_{254} indicator. Spectra were measured in DMSO–d_6 on a Bruker AV-400 spectrometer (400 MHz for ^{1}H, 100 MHz for ^{13}C, and 40.54 MHz for ^{15}N), purchased with assistance from the National Science Foundation (CHE 03–42,251) at the Florida Institute of Technology, 150 W University Blvd, Melbourne, FL 32,901, USA. Chemical shifts are reported *vs* TMS = 0 for ^{1}H and ^{13}C, and *vs* NH_3 = 0 for ^{15}N. ^{15}N signals were detected indirectly, *via* HSQC and HMBC experiments. The samples were dissolved in DMSO–d_6, *s* = singlet, *d* = doublet, dd = doublet of doublet and *t* = triplet. Mass spectrometry were recorded on a Varian MAT 312 instrument in EI mode (70 eV), at the Karlsruhe Institut für Technologie (KIT), Institute of Organic Chemistry, Karlsruhe, Germany.

Synthesis of substituted *(E)-N'*-(substituted benzylidene)−2-((7-substituted-2-oxo-1,2-dihydroquinolin-4-yl)oxy)acetohydrazide **4a-**k.

A mixture of **3a,b** (1 mmol), aldehydes (1 mmol) and a few drops of acetic acid in 20 mL of absolute ethanol which was stirred and refluxed for 6–8 h (the reaction was followed by TLC analysis). After the reaction's completion, the solid was filtered off and washed with a hot ethanol to give pure compounds **4a-**k.

(*E*)-*N*'-Benzylidene-2-((7-methyl-2-oxo-1,2-dihydroquinolin-4-yl)oxy)acetohydrazide (**4a**).

This compound was obtained as a colorless compound, yield 0.28 g (83%); R_f = 0.4 (Toluene: Ethyl acetate; 10:1); ^{1}H NMR (DMSO–d_6): δ_H = 11.75 (s; 1H, NH, H-4e), 11.34 (s; 1H, NH-1), 8.04 (s; 1H, H-4 g), 7.76 (m; 3H, H-5,*o*), 7.45 (m; 3H, H-*m*,*p*), 7.09 (s; 1H, H-8), 7.04 (d; *J* = 8.2, 1H, H-6), 5.73 (s; 1H, H-3), 5.34 (s; 2H, H-4c), 2.38 (s; 3H, H-7a); ^{13}C NMR (DMSO–d_6): δ_c = 167.78 (C-4d), 163.25 (C-2), 162.08 (C-4), 144.13 (C-4 g), 141.07 (C-7), 140.15 (C-8a), 133.89 (C-*i*), 129.98 (C-*p*), 127.75 (C-*m*), 126.99 (C-*o*), 122.76 (C-6), 122.35 (C-5), 114.87 (C-8), 112.38 (C-4a), 96.64 (C-3), 65.14 (C-4c), 21.28 (C-7a); ^{15}N NMR (DMSO–d_6): δ_N = 315.1 (N-4f), 177.4 (N-4e), 144.1 (N-1a). MS (70 eV): *m/z* (%) = 335 (M^+, 60). Anal. Calcd for $C_{19}H_{17}N_3O_3$ (335.36): C 68.05; H 5.11; N 12.53. Found: C 68.1;, H 4.99; N 12.66.

(*E*)-*N*'-(4-Bromobenzylidene)−2-((7-methyl-2-oxo-1,2-dihydroquinolin-4-yl)oxy)-acetohydrazide (**4b**).

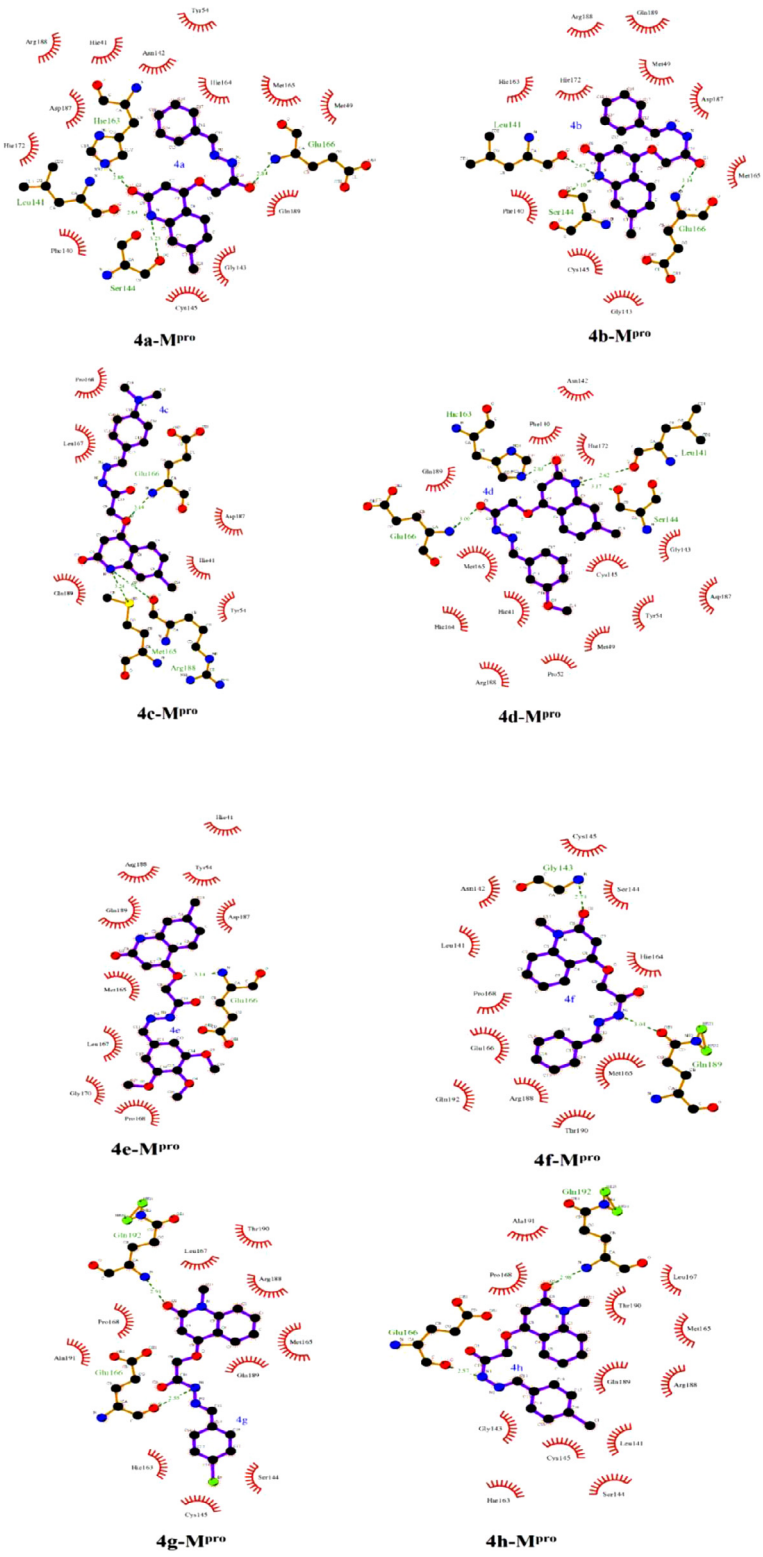

Fig. 7. 2D LigPlus representation of interactions of compounds **4a-k** with important amino acid residues of SARS-CoV-2 main protease (M^{pro}).

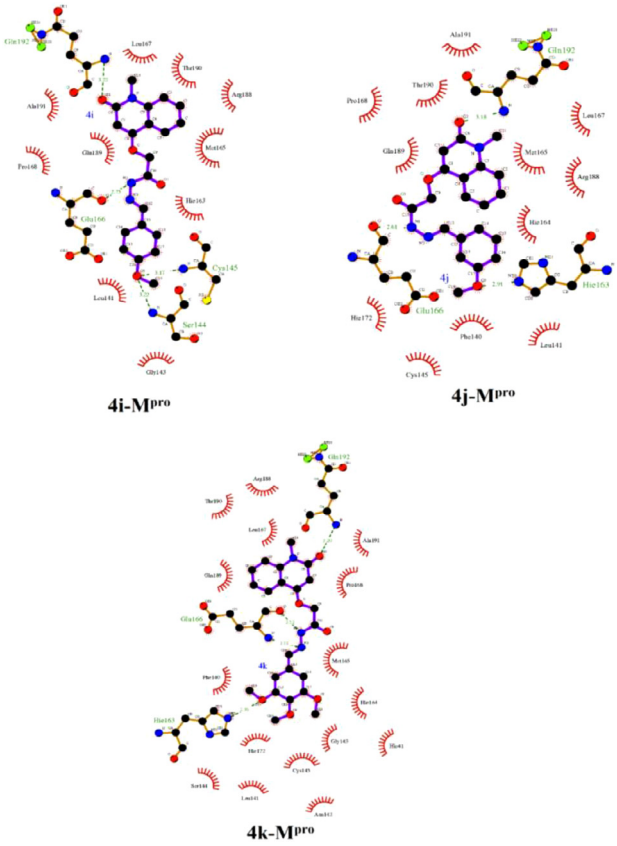

Fig. 7. Continued

This compound was obtained as a colorless compound, yield 0.300 g (72%); R_f = 0.3 (Toluene: Ethyl acetate; 10:1); NMR (DMSO–d_6): δ (See Tables 1 and 2). MS (70 eV): *m/z* (%) = 415 (M + 1, 36), 414 (M^+, 32). Anal. Calcd for $C_{19}H_{16}BrN_3O_3$ (414.25): C 55.09; H 3.89; N 10.14. Found: C 55.10; H 3.77; N 10.11.

(*E*)-*N*′-(4-(Dimethylamino)benzylidene)−2-((7-methyl-2-oxo-1,2-dihydroquinolin-4-yl)oxy)-acetohydrazide (**4c**).

This compound was obtained as a colorless compound, yield 0.300 g (79%); R_f = 0.6 (Toluene: Ethyl acetate; 10:1); ^{1}H NMR (DMSO–d_6): δ_H = 11.45 (s; 1H, NH, H-4e), 11.33 (s; 1H, NH-1), 7.90 (s; 1H, H-4 g), 7.76 (d, *J* = 8.2 Hz; 1H, H-5), 7.54 (d, *J* = 8.86 Hz; 2H, H-*o*), 7.09 (s; 1H, H-8), 7.03 (d, *J* = 8.3 Hz; 1H, H-6), 6.75 (d, *J* = 8.8 Hz; 2H, H-*m*), 5.68 (s; 1H, H-3), 5.28 (s; 2H, H-4c), 2.98 (s; 6H, NMe_2), 2.38 (s; 3H, H-7a); ^{13}C NMR (DMSO–d_6): δ_c = 167.12 (C-4d), 163.25 (C-2), 162.14 (C-4), 151.45 (C-*p*), 144.95 (C-4 g), 141.07 (C-7), 140.15 (C-8a), 128.51, 128.25 (C-*o*,*i*), 122.75 (C-6), 122.36 (C-5), 114.87 (C-8), 112.40 (C-4a), 111.74 (C-*m*), 96.56 (C-3), 65.13 (C-4c), 39.50 (NMe_2), 21.28 (C-7a); ^{15}N NMR (DMSO–d_6): δ_N = 303.6 (N-4f), 176.4 (N-4e), 144.0 (N-1a), 52.8 (NMe_2). MS (70 eV): *m/z* (%) = 378 (M^+, 60). Anal. Calcd for $C_{21}H_{22}N_4O_3$ (378.42): C 66.65; H 5.86; N 14.81. Found: C 66.77; H 5.79; N 14.66.

(*E*)-*N*′-(3-Methoxybenzylidene)−2-((7-methyl-2-oxo-1,2-dihydroquinolin-4-yl)oxy)acetohydrazide (**4d**).

This compound was obtained as a colourless compound, yield 0.280 g (77%); R_f = 0.65 (Toluene: Ethyl acetate; 10:1); ^{1}H NMR (DMSO–d_6): δ_H = 11.76 (s; 1H, NH, H-4e), 11.34 (s; 1H, NH-1), 8.00 (s; 1H, H-4 g), 7.76 (d; *J* = 8.2 Hz, 1H, H-5), 7.37 (m; 1H, H-5′), 7.30, (m; 2H, H-2′,6′), 7.09 (s; 1H, H-8), 7.02 (m; 2H, H-4′,6′), 5.72 (s; 1H, H-3), 5.35 (s; 2H, H-4c), 3.80 (s; 3H, H-3a), 2.38 (s; 3H, H-7a); ^{13}C NMR (DMSO–d_6): δ_c = 167.83 (C-4d), 163.24 (C-2), 162.09 (C-4), 159.51 (C-3′), 143.94 (C-4 g), 141.21 (C-7), 140.15 (C-8a), 135.31 (C-1′), 129.86 (C-5′), 122.76 (C-6), 122.33 (C-5), 119.68 (C-6′), 115.94 (C-5′), 114.88 (C-8), 112.39 (C-4a), 111.64 (C-2′), 96.66 (C-3), 65.19 (C-4c), 55.15 (C-3a'), 21.27 (C-7a); ^{15}N NMR (DMSO–d_6): δ_N = 316.1 (N-4f), 177.5 (N-4e), 144.3 (N-1a). MS (70 eV): *m/z* (%) = 365 (M^+, 27). Anal. Calcd for $C_{20}H_{19}N_3O_4$ (365.38): C 65.74; H 5.24; N 11.50. Found: C 65.66; H 5.09; N 11.44.

(*E*)−2-((7-Methyl-2-oxo-1,2-dihydroquinolin-4-yl)oxy)-*N*′-(3,4,5-trimethoxybenzylidene)aceto-hydrazide (**4e**).

This compound was obtained as a colorless compound, yield 0.38 g (90%); R_f = 0.45 (Toluene: Ethyl acetate; 10:1); ^{1}H NMR (DMSO–d_6): δ_H = 11.78 (s; 1H, NH, H-4e), 11.34 (s; 1H, NH-1), 7.95 (s; 1H, H-4 g), 7.76 (d; *J* = 8.2 Hz, 1H, H-5), 7.09 (s; 1H, H-8), 7.05 (m; 3H, H-2′,6), 5.70 (s; 1H, H-3), 5.37 (s; 2H, H-4c), 3.81 (s; 3H, H-3a',5a'), 2.89 (s; 3H, H-4a'), 2.38 (s; 3H, H-7a); ^{13}C NMR (DMSO–d_6): δ_c = 167.81 (C-4d), 163.24 (C-2), 162.13 (C-4), 153.12 (C-3′), 143.92 (C-4 g), 141.06 (C-7), 140.15 (C-8a), 138.80 (C-4′), 129.40 (C-1′), 122.77 (C-6), 122.31 (C-5), 114.88 (C-8), 112.38 (C-4a), 104.34 (C-2′), 96.64 (C-3), 60.08 (C-4c), 55.92 (C-4a'), 35.73 (C-3a'), 21.26 (C-7a); ^{15}N NMR (DMSO–d_6): δ_N = 313.2 (N-4f), 177.5 (N-4e), 143.9 (N-1a). MS (70 eV): *m/z* (%) = 425 (M^+, 55). Anal. Calcd for $C_{22}H_{23}N_3O_6$ (425.43): C 62.11; H 5.45; N 9.88. Found: C 62.28; H 5.59; N 10.01.

(*E*)-*N*′-Benzylidene-2-((1-methyl-2-oxo-1,2-dihydroquinolin-4-yl)oxy)acetohydrazide (**4f**).

This compound was obtained as a colorless compound, yield 0.275 g (82%); R_f = 0.5 (Toluene: Ethyl acetate; 10:1); ^{1}H NMR (DMSO–d_6): δ_H = 11.75 (s; 1H, NH, H-4e), 8.04 (s; 1H, H-4 g), 8.01 (d, *J* = 7.8 Hz; 1H, H-8), 7.76 (dd, *J* = 7.8, 2.2 Hz; 2H, H-*o*), 7.69 (m; 1H, H-7), 7.54 (d, *J* = 8.5 Hz; 1H, H-5), 7.46 (m; 3H, H-*m*,*p*), 7.31 (m; 1H, H-6), 5.98 (s; 1H, H-3), 5.38 (s; 2H, H-4c), 3.58 (s; 3H, H-1a); ^{13}C NMR (DMSO–d_6): δ_c = 167.71 (C-4d), 162.17 (C-2), 160.65 (C-4), 144.16 (C-4 g), 139.47 (C-8a), 133.89 (C-*i*), 131.48 (C-7), 129.98 (C-*p*), 128.75 (C-*m*), 127.01 (C-*o*), 122.88 (C-

8), 121.55 (C-6), 115.56 (C-4), 114.64 (C-5), 97.21 (C-3), 65.28 (C-4c), 28.62 (C-1a); ^{15}N NMR (DMSO–d_6): δ_N = 315.1 (N-4f), 177.8 (N-4e), 137.4 (N-1a). MS (70 eV): *m/z* (%) = 335 (M^+, 45). Anal. Calcd for $C_{19}H_{17}N_3O_3$ (335.36): C 68.05; H 5.11; N 12.53. Found: C 68.16; H 4.99; N 12.39.

(*E*)-*N*′-(4-Bromobenzylidene)−2-((1-methyl-2-oxo-1,2-dihydroquinolin-4-yl)oxy)acetohydrazide **(4g)**.

This compound was obtained as a colorless compound, yield 0.290 g (70%); R_f = 0.3 (Toluene: Ethyl acetate; 10:1); ^{1}H NMR (DMSO–d_6): δ_H = 11.81 (s; 1H, NH, H-4e), 8.01 (s; 2H, H-4 g,8), 7.72 (d, *J* = 8.5 Hz; 2H, H-o), 7.64 (m; 3H, H-7,*m*), 7.54 (d, *J* = 8.5 Hz; 1H, H-5), 7.31 ("t", *J* = 7.5 Hz; 1H, H-6), 5.99 (s; 1H, H-3), 5.37 (s; 2H, H-4c), 3.57 (s; 3H, H-1a); ^{13}C NMR (DMSO–d_6): δ_c = 167.80 (C-4d), 162.17 (C-2), 160.61 (C-4), 142.96 (C-4 g), 139.46 (C-8a), 133.20 (C-*i*), 131.73 (C-*m*), 131.48 (C-7), 128.91 (C-*o*), 123.21 (C-*p*), 122.86 (C-8), 121.55 (C-6), 114.64 (C-5), 97.23 (C-3), 65.27 (C-4c), 28.62 (C-1a); ^{15}N NMR (DMSO–d_6): δ_N = 316.9 (N-4f), 178.1 (N-4e), 137.4 (N-1a). MS (70 eV): *m/z* (%) = 415 (M + 1, 28), 414 (M^{+}, 33). Anal. Calcd for $C_{19}H_{16}BrN_3O_3$ (414.25): C 55.09; H 3.89; Br 19.29; N 10.14. Found: C 55.17; H 3.99; Br 19.33; N 10.20.

(*E*)-*N*′-(4-Chlorobenzylidene)−2-((1-methyl-2-oxo-1,2-dihydroquinolin-4-yl)oxy)-acetohydrazide (**4h**).

This compound was obtained as a colorless compound, yield 0.288 g (78%); R_f = 0.35 (Toluene: Ethyl acetate; 10:1); ^{1}H NMR (DMSO–d_6): δ_H = 11.81 (s; 1H, NH, H-4e), 8.02 (m; 2H, H-4 g,8), 7.79 (d, *J* = 8.4 Hz; 2H, H-*o*), 7.75 (d, *J* = 8.4 Hz; 1H, H-5), 7.68 ("t", *J* = 7.7 Hz; 1H, H-7), 7.31 ("t", *J* = 7.5 Hz; 1H, H-6), 5.99 (s; 1H, H-3), 5.37 (s; 2H, H-4c), 3.57 (s; 3H, H-1a); ^{13}C NMR (DMSO–d_6): δ_c = 167.79 (C-4d), 162.18 (C-2), 160.62 (C-4), 142.86 (C-4 g), 139.46 (C-8a), 134.43 (C-*p*), 132.86 (C-*i*), 131.47 (C-7), 128.81, 128.68 (C-*o*,5), 122.86 (C-8), 121.53 (C-6), 115.55 (C-4a), 97.22 (C-3), 65.28 (C-4c), 28.62 (C-1a); ^{15}N NMR (DMSO–d_6): δ_N = 316.9 (N-4f), 177.9 (N-4e), 137.2 (N-1a). MS (70 eV): *m/z* (%) = 371 (M + 1, 27), 370 (M^+, 30). Anal. Calcd for $C_{19}H_{16}ClN_3O_3$ (369.80): C 61.71; H 4.36; Cl 9.59; N 11.36. Found: C 61.77; H 4.44; Cl 9.65; N 11.45.

(*E*)-*N*′-(4-Methoxybenzylidene)−2-((1-methyl-2-oxo-1,2-dihydroquinolin-4-yl)-oxy)acetohydrazide (**4i**).

This compound was obtained as a colorless compound, yield 0.260 g (71%); R_f = 0.6 (Toluene: Ethyl acetate; 10:1); ^{1}H NMR (DMSO–d_6): δ_H = 11.62 (s; 1H, NH, H-4e), 8.01 (dd, *J* = 8.0, 1.3 Hz; 1H, H-8), 7.98 (s; 1H, H-4 g), 7.70 (d, *J* = 8.7 Hz; 2H, H-*o*), 7.67 (m; 1H, H-7), 7.54 (d, *J* = 8.5 Hz; 1H, H-5), 7.32 (m; 1H, H-6), 7.01 (d, *J* = 8.8 Hz; 2H, H-*m*), 5.96 (s; 1H, H-3), 5.35 (s; 2H, H-4c), 3.81 (s; 3H, OMe), 3.58 (s; 3H, H-1a); ^{13}C NMR (DMSO–d_6): δ_C = 167.44 (C-4d), 162.17 (C-2), 160.76, 160.67 (C-4*p*), 144.03 (C-4 g), 139.47 (C-8a), 131.48 (C-7), 128.60 (C-*o*), 126.51 (C-*i*), 122.88 (C-8), 121.56 (C-6), 115.56 (C-4a), 114.64 (C-5), 114.26 (C-*m*), 97.18 (C-3), 65.27 (C-4c), 55.28 (OMe), 28.62 (C-1a); ^{15}N NMR (DMSO–d_6): δ_N = 308.6 (N-4f), 176.7 (N-4e), 137.3 (N-1a). MS (70 eV): *m/z* (%) = 365 (M^+, 30). Anal. Calcd for $C_{20}H_{19}N_3O_4$ (365.38): C 65.74; H 5.24; N 11.50. Found: C 65.77; H 5.33; N 11.44.

(*E*)-*N*′-(3-Methoxybenzylidene)−2-((1-methyl-2-oxo-1,2-dihydroquinolin-4-yl)-oxy)acetohydrazide (**4j**).

This compound was obtained as a colorless compound, yield 0.277 g (76%); R_f = 0.65 (Toluene: Ethyl acetate; 10:1); ^{1}H NMR (DMSO–d_6): δ_H = 11.77 (s; 1H, NH, H-4e), 8.00 (m; 2H, H-4 g,8), 7.69 (ddd, *J* = 8.5, 7.1, 1.4 Hz; 1H, H-7), 7.54 (d, *J* = 8.5 Hz; 1H, H-5), 7.37 ("t", *J* = 7.9 Hz; 1H, H-5′), 7.31 (m; 3H, H-6,2′,6′), 7.00 (m; 1H, H-4′), 5.97 (s; 1H, H-3), 5.39 (s; 2H, H-4c), 3.80 (s; 3H, OMe), 3.58 (s; 3H, H-1a); ^{13}C NMR (DMSO–d_6): δ_C = 167.77 (C-4d), 162.16 (C-2), 160.66 (C-4), 159.51 (C-3′), 143.98 (C-4 g), 139.46 (C-8a), 135.31 (C-1′), 131.48 (C-7), 129.85 (C-5′), 122.86 (C-8), 121.55 (C-6), 119.68 (C-6′), 115.91 (C-4′), 115.55 (C-4a), 114.64 (C-5), 111.70 (C-2′), 97.22 (C-3), 65.33 (C-4c), 55.15 (C-3a'), 28.62 (C-1a); ^{15}N NMR (DMSO–d_6): δ_N = 315.8 (N-4f), 177.7 (N-4e), 137.4 (N-1a). MS (70 eV): *m/z* (%) = 365 (M^+, 65). Anal. Calcd for $C_{20}H_{19}N_3O_4$ (365.38): C 65.74; H 5.24; N 11.50. Found: C 65.70; H 5.33; N 11.40.

(*E*)−2-((1-Methyl-2-oxo-1,2-dihydroquinolin-4-yl)oxy)-*N*′-(3,4,5-trimethoxy-benzylidene)aceto-hydrazide (**4k**).

This compound was obtained as a colorless compound, yield 0.325 g (76%); R_f = 0.35 (Toluene: Ethyl acetate; 10:1); ^{1}H NMR (DMSO–d_6): δ_H = 11.78 (s; 1H, NH, H-4e), 8.00 (d, *J* = 7.9 Hz; 1H, H-8), 7.95 (s; 1H, H-4 g), 7.69 ("t", *J* = 7.8 Hz; 1H, H-7), 7.54 (d, *J* = 8.6 Hz; 1H, H-5), 7.37 ("t", *J* = 7.9 Hz; 1H, H-5′), 7.32 (m; 1H, H-6), 7.05 (s; 2H, H-2′), 5.95 (s; 1H, H-3), 5.41 (s; 2H, H-4c), 3.83 (s; 6H, H-3a'), 3.70 (s; 3H, H-4a'), 3.58 (s; 3H, H-1a'); ^{13}C NMR (DMSO–d_6): δ_C = 167.75 (C-4d), 162.15 (C-2), 160.71 (C-4), 153.13 (C-3′), 143.96 (C-4 g), 139.47 (C-8a,4′), 131.48 (C-7), 129.40 (C-1′), 122.85 (C-8), 121.55 (C-6), 115.56 (C-4a), 114.64 (C-5), 97.21 (C-3), 65.40 (C-4c), 60.09 (C-4a'), 55.95 (C-3a'), 28.62 (C-1a); ^{15}N NMR (DMSO–d_6): δ_N = 313.2 (N-4f), 177.2 (N-4e), 137.2 (N-1a). MS (70 eV): *m/z* (%) = 425 (M^+, 45). Anal. Calcd for $C_{22}H_{23}N_3O_6$ (425.43): C 62.11; H 5.45; N 9.88. Found: C 62.20; H 5.39; N 9.76.

5. Molecular docking calculations

The crystal structures of SARS-CoV-2 main protease (M^{pro}; PDB code: 6LU7 [46]) and RNA-dependent RNA polymerase (RdRp; PDB code: 6M71 [47]) were taken as templates for all molecular docking. Receptors were cleaned of water molecules, ions and the ligands. The protonation state of M^{pro} and RdRp was investigated using an H^{++} server, and all missing hydrogen atoms were added [48]. All molecular docking calculations were carried out using Autodock4.2.6 software [49]. All docking parameters were kept to default values, except the number of genetic algorithm (*GA*) runs and the maximum number of energy evaluations (*eval*) which were set to 250 and 25,000,000, respectively. The docking grid was set to 60Å x 60Å x 60Å with a grid spacing value of 0.375 Å, and the grid center was placed at the center of the active site. The geometrical structures of all synthesized compounds were minimized with a MMFF94s force field using SZYBKI software [50] and the partial atomic charges were assigned using the Gasteiger method [51].

CRediT author statement and authorship

I would like to confirm and certify the authors' contributions as indicated in the followings:

Mohammed B Alshammari (Writing-review & editing, Funding acquisition)

Mohamed Ramadan (Supervision, Writing-review & editing)

Ashraf A Aly (Conceptualization, Superivsion, Writing-original draft, Writing-review & editing)

Essmat M. El-Sheref (Methodology, Writing-review & editing)

Md Afroz Bakht (Visualization)

Mahmoud A. A. Ibrahim (Methodology, Writing-review & editing)

Ahmed M. Shawky (Validation_Visualization)

Declaration of Competing Interest

The authors declare that they have no known competing financial interests or personal relationships that could have appeared to influence the work reported in this paper.

Acknowledgement

The authors thank the Deanship of Scientific Research at Prince Sattam Bin Abdulaziz University under the research project No10302/1/2019.

Supplementary materials

Supplementary material associated with this article can be found, in the online version, at doi:10.1016/j.molstruc.2020.129649.

References

[1] Y.S. Malik, S. Sircar, S. Bhat, K. Sharun, K. Dhama, M. Dadar, R. Tiwari, W. Chaicumpa, Emerging novel coronavirus (2019-nCoV)-current scenario, evolutionary perspective based on genome analysis and recent developments, Vet. Q. 40 (1) (2020) 68–76, doi:10.1080/01652176.2020.1727993.

[2] P.I. Lee, P.R. Hsueh, Emerging threats from zoonotic coronaviruses-from SARS and MERS to 2019-nCoV, J. Microbiol. Immunol. Infect. (2020) (in press), doi:10.1016/j.jmii.2020.02.00.

[3] L. Du, Y. He, Y. Zhou, S. Liu, B.J. Zheng, S. Jiang, The spike protein of SARS-CoV-a target for vaccine and therapeutic development, Nat. Rev. Microbiol. 7 (3) (2009) 226–236, doi:10.1038/nrmicro2090.

[4] D. Wrapp, N. Wang, K.S. Corbett, J.A. Goldsmith, C.L. Hsieh, O. Abiona, B.S. Graham, J.S. McLellan, Cryo-EM structure of the 2019-nCoV spike in the prefusion conformation, Science 367 (6483) (2020) 1260–1263, doi:10.1126/science.abb2507.

[5] M. Hoffmann, H. Kleine-Weber, S. Schroeder, N. Krüger, T. Herrler, S. Erichsen, T.S. Schiergens, G. Herrler, N.-.H. Wu, A. Nitsche, M.A. Müller, C. Drosten, S. Pöhlmann, SARS-CoV-2 Cell Entry Depends on ACE2 and TMPRSS2 and is Blocked by a Clinically Proven Protease Inhibitor, Cell (2020) in press, doi:10.1016/j.cell.2020.02.052.

[6] S.J. Anthony, C.K. Johnson, D.J. Greig, S. Kramer, X. Che, H. Wells, A.L. Hicks, D.O. Joly, N.D. Wolfe, P. Daszak, W. Karesh, W.I. Lipkin, S.S. Morse, P. Consortium, J.A.K. Mazet, T. Goldstein, Global patterns in coronavirus diversity, Virus Evol 3 (1) (2017) vex012., doi:10.1093/ve/vex012.

[7] K. Anand, J. Ziebuhr, P. Wadhwani, J.R. Mesters, R. Hilgenfeld, Coronavirus main proteinase (3CLpro) structure: basis for design of anti-SARS drugs, Science 300 (5626) (2003) 1763–1767, doi:10.1126/science.1085658.

[8] F. Wang, C. Chen, W. Tan, K. Yang, H. Yang, Structure of Main Protease from Human Coronavirus NL63: insights for Wide Spectrum Anti-Coronavirus Drug Design, Sci. Rep. 6 (2016) 22677, doi:10.1038/srep22677.

[9] Du Y.X., Chen X.-.P., Favipiravir: pharmacokinetics and concerns about clinical trials for 2019-nCoV infection, Clin Pharmacol Ther 2006 (in press) 10.1002/cpt.1844.

[10] T.P. Sheahan, A.C. Sims, R.L. Graham, V.D. Menachery, L.E. Gralinski, J.B. Case, S.R. Leist, K. Pyrc, J.Y. Feng, I. Trantcheva, R. Bannister, Y. Park, D. Babusis, M.O. Clarke, R.L. Mackman, J.E. Spahn, C.A. Palmiotti, D. Siegel, A.S. Ray, T. Cihlar, R. Jordan, M.R. Denison, R.S. Baric, Broad-spectrum antiviral GS-5734 inhibits both epidemic and zoonotic coronaviruses, Sci. Transl. Med. 9 (396) (2017) l3653, doi:10.1126/scitranslmed.aal3653.

[11] S. Mulangu, L.E. Dodd, R.T. Davey, O.T. Mbaya, M. Proschan, D. Mukadi, M.L. Manzo, D. Nzolo, A.T. Oloma, A. Ibanda, R. Ali, S. Coulibaly, A Randomized, Controlled Trial of Ebola Virus Disease Therapeutics, N. Engl. J. Med. 381 (2019) 2293–2303, doi:10.1056/NEJMoa1910993.

[12] M. Wang, R. Cao, L. Zhang, X. Yang, J. Liu, M. Xu, Z. Shi, Z. Hu, W. Zhong, G. Xiao, Remdesivir and chloroquine effectively inhibit the recently emerged novel coronavirus (2019-nCoV, in vitro. Cell Res 30 (3) (2020) 269–271, doi:10.1038/s41422-020-0282-0.

[13] I.A. Bessonova, Components of Haplophyllum bucharicum, Chem. Nat. Compds 36 (2000) 323–324.

[14] A. Detsi, V. Bardakaos, J. Markopoulos, O. Igglessi-Markopoulou, Reactions of 2-methyl-3,1-benzoxazin-4-one with active methylene compounds: a new route to 3-substituted 4-hydroxyquinolin-2(1*H*)-ones, J. Chem. Sec. Perkin. Trans 1 (1996) 2909–2913, doi:10.1039/P19960002909.

[15] V.I. Ukrainets, N.L. Bereznyakova, E.V. Mospanova, 4-Hydroxy-2-quinolones 121. Synthesis and biological properties of 1-hydroxy-3-oxo-5,6-dihydro-3H-pyrrolo[3,2,1-*ij*]quinoline-2 carboxylic acid alkyl amides, Chem. Heterocycl. Compds. 43 (2007) 856–862, doi:10.1007/s10593-007-0136-4.

[16] J.L. McCormick, T.C. McKee, J.H. Cardinella, M.R. Boyd, HIV Inhibitory Natural Products. Quinoline Alkaloids from Euodia roxburghiana, J. Nat. Prod. 59 (5) (1996) 469–471.

[17] P. Luthra, J. Liang, C.A. Pietzsch, S. Khadka, M.R. Edwards, S. Wei, S. De, B. Posner, A. Bukreyev, J.M. Ready, C.F. Basler, A high throughput screen identifies benzoquinoline compounds as inhibitors of Ebola virus replication, Antivir. Res. 150 (2018) 193–201, doi:10.1016/j.antiviral.2017.12.019.

[18] A. Loregian, B. Mercorelli, G. Muratore, E. Sinigalia, S. Pagni, S. Massari, G. Gribaudo, B. Gatto, M. Palumbo, O. Tabarrini, V. Cecchetti, G. Palu, The 6-aminoquinolone WC5 inhibits human cytomegalovirus replication at an early stage by interfering with the transactivating activity of viral immediate-early protein, Antimicrob. Agents Chemother. 54 (5) (2010) 1930–1940, doi:10.1128/AAC.01730-09.

[19] D. Plantone, T. Koudriavtseva, Current and future use of chloroquine and hydroxychloroquine in infectious, immune, neoplastic, and neurological diseases: a mini-review, Clin. Drug Investig. 38 (8) (2018) 653–671, doi:10.1007/s40261-018-0656-y.

[20] G. Barbosa-Lima, A.M. Moraes, A.D.S. Araujo, E.T. da Silva, C.S. de Freitas, Y.R. Vieira, A. Marttorelli, J.C. Neto, P.T. Bozza, M.V.N. de Souza, T.M.L. Souza, 2,8-bis(trifluoromethyl)quinoline analogs show improved anti-Zika virus activity, compared to mefloquine, Eur. J. Med. Chem. 127 (2017) 334–340, doi:10.1016/j.ejmech.2016.12.058.

[21] M.A. Al-Bari, Chloroquine analogues in drug discovery: new directions of uses, mechanisms of actions and toxic manifestations from malaria to multifarious diseases, J. Antimicrob. Chemother. 70 (6) (2015) 1608–1621, doi:10.1093/jac/dkv018.

[22] R. Delvecchio, Higa, L.M. Pezzuto, P. Valadao, A.L. Garcez, P.P. Monteiro, F.L. Loiola, E.C. Dias, A.A. Silva, F.J. Aliota, M.T. Caine, E.A. Osorio, J.E. Bellio, M. O'Connor, D.H. Rehen, S. de Aguiar, R.S. Savarino, A. Campanati, L. Tanuri, A. Chloroquine, an endocytosis blocking agent, inhibits Zika virus infection in different cell models, Viruses 8 (12) (2016) 322, doi:10.3390/v8120322.

[23] S. Richter, C. Parolin, M. Palumbo, G. Palù, Antiviral Properties of Quinolone-based Drugs, Curr Drug Target – Infect Disord 4 (2004) 111–116, doi:10.2174/1568005043340920.

[24] A. Savarino, J.R. Boelaert, A. Cassone, G. Majori, R. Cauda, Effects of chloroquine on viral infections: an old drug against today's diseases, Lancet Infect Dis 3 (2003) 722–727, doi:10.1016/s1473-3099(03)00806-5.

[25] M. Sato, T. Motomura, H. Aramaki, T. Matsuda, M. Yamashita, Y. Ito, H. Kawakami, Y. Matsuzaki, W. Watanabe, K. Yamataka, S. Ikeda, E. Kodama, M. Matsuoka, H. Shinkai, Novel HIV-1 integrase inhibitors derived from quinolone antibiotics, J. Med. Chem. 49 (5) (2006) 1506–1508, doi:10.1021/jm0600139.

[26] Z. Hajimahdi, R. Zabihollahi, M.R. Aghasadeghi, S. Hosseini-Ashtiani, A. Zargh, Novel quinolone-3-carboxylic acid derivatives as anti-HIV-1 agents: design, synthesis, and biological activities, Med. Chem. Res. 25 (2016) 1861–1876, doi:10.1007/s00044-016-1631-x.

[27] A.A. Aly, E.M. El-Sheref, A.F.E. Mourad, M.E.M. Bakheet, S. Bräse, M. Nieger, One-pot synthesis of 2,3-bis-(4-hydroxy-2-oxo-1,2-dihydroquinolin-3-yl)succinates and arylmethylene-bis-3,3′-quinoline-2-ones, Chem Pap 73 (2019) 27–37.

[28] A.A. Aly, M. Ramadan, A.A.M. El-Reedy, Reactions of 4-hydroxyquinolin-2(1*H*)-ones with acenaphthoquinone: synthesis of new 1,2-dihydroacenaphthylene-spiro-tetrakis(4-hydroxy-quinolin-2(1*H*)-ones), J. Heterocycl. Chem. 56 (2019) 642–645.

[29] A.A. Aly, E.M. El-Sheref, A.-F.E. Mourad, A.B. Brown, S. Bräse, M.E.M. Bakheet, M. Nieger, Synthesis of spiro[indoline-3,4′-pyrano[3,2-*c*]quinolone]-3′-carbonitriles, Monatsh. Chem 149 (2018) 635–644.

[30] E.M. El-Sheref, A.A. Aly, A.-F.E. Mourad, A.B. Brown, S. Bräse, M.E.M. Bakheet, Synthesis of pyrano[3,2-*c*]quinoline-4-carboxylates and 2-(4-oxo-1,4-dihydroquinolin-3-yl)fumarates, Chem. Pap. 72 (2018) 181–190.

[31] E.M. El-Sheref, A.A. Aly, M.A. Ameen, A.B. Brown, New 4-(1,2,3-triazolo)quinolin-2(1*H*)-ones *via* Cu-catalyzed [3+2] cycloaddition, Monatsh. Chem 150 (2019) 747–756.

[32] A.A. Aly, E.M. El-Sheref, M.E.M. Bakheet, M.A.E. Mourad, S. Bräse, M.A.A. Ibrahim, M. Nieger, B.K. Garvalov, K.N. Dalby, T.S Kaoud, Design, synthesis and biological evaluation of fused naphthofuro[3,2-*c*]quinoline-6,7,12-triones and pyrano[3,2-*c*]quinoline-6,7,8,13-tetraones derivatives as ERK inhibitors with efficacy in BRAF-mutant melanoma, Bioorg. Chem 82 (2019) 290–305.

[33] A.A. Aly, E.M. El-Sheref, M.E.M. Bakheet, M.A.E. Mourad, A.B. Brown, S. Bräse, M. Nieger, M.A.A. Ibrahim, Synthesis of novel 1,2-bis-quinolinyl-1,4-naphthoquinones: ERK2 inhibition, cytotoxicity and molecular docking studies, Bioorg. Chem. 81 (2018) 700–712.

[34] A.A. Aly, A.A. Hassan, N.K. Mohamed, S. Bräse, L.E. Abd El-Haleem, M. Polamo, M. Nieger, A.B. Brown, Synthesis of new fused heterocyclic 2-quinolones and 3-alkanonyl-4-hydroxy-2-quinolones, Molecules 24 (2020) 3782–3795.

[35] M.A.I. Elbastawesy, Ramadan M.El-Shaier, Aly A.A. Y.A.A.M., A. El-Din, G. Abuo-Rahma, Arylidenes of Quinolin-2-one scaffold as Erlotinib analogues with activities against leukemia through inhibition of EGFR TK/ STAT-3 pathways, Biorg. Chem. 96 (2020) 103628.

[36] S.M. Sondhi, N. Singh, A. Kumar, O. Lozach, L Meijer, Synthesis, anti-inflammatory, analgesic and kinase (CDK-1,CDK-5 and GSK-3) inhibition activity evaluation of benzimidazole/benzoxazole derivatives and some Schiff's bases, Bioorg. Med. Chem. 14 (11) (2006) 3758–3765, doi:10.1016/j.bmc.2006.01.054.

[37] A. Pandey, D. Dewangan, S. Verma, A. Mishra, R.D. Dubey, Synthesis of Schiff bases of 2-amino-5-aryl-1,3,4-thiadiazole And its Analgesic, AntiInflammatory, Anti-Bacterial and Antitubercular Activity, Inter. J. Chem. Tech. Res. 3 (1) (2011) 178–184.

[38] S.M.R. Chandramouli, T.B. Nayanbhai, R.H. Bheemachari Udupi, Synthesis and biological screening of certain new triazole schiff bases and their derivatives bearing substituted benzothiazole moiety, J. Chem. Pharm. Res. 4 (2) (2012) 1151–1159.

[39] R.P. Chinnasamy, R. Sundararajan, S Govindaraj, Synthesis, characterization, and analgesic activity of novel Schiff base of isatin derivatives, J. Adv. Pharm. Tech. Res. 1 (3) (2010) 342–347, doi:10.4103/0110-5558.72428.

[40] B.S. Sathe, E. Jaychandran, V.A. Jagtap, G.M. Sreenivasa, Synthesis characterization and anti-inflammatory evaluation of new fluorobenzothiazole schiff's bases, Inter. J. Pharm. Res. Develop. 3 (3) (2011) 164–169.

[41] T. Aboul-Fadl, F.A. Mohammed, E.A. Hassan, Synthesis, antitubercular activity and pharmacokinetic studies of some Schiff bases derived from 1-alkylisatin and isonicotinic acid hydrazide (INH), Arch. Pharm. Res. 26 (10) (2003) 778–784, doi:10.1007/BF02980020.

[42] R. Miri, N. Razzaghi-Asl, M.K. Mohammadi, QM study and conformational analysis of an isatin Schiff base as a potential cytotoxic agent, J. Molecul. Mod. 19 (2) (2013) 727–735, doi:10.1007/s00894-012-1586-x.

[43] S.M.M. Ali, M.A.K. Azad, M. Jesmin, S. Ahsan, M.M. Rahman, J.A. Khanam, M.N. Islam, S.M.S. Shahria, *In vivo* anticancer activity of vanillin semicarbazone, Asian Pacific J. Trop. BioMed. 2 (6) (2012) 438–442, doi:10.1016/S2221-1691(12)60072-0.
[44] S.S. Panda, R. Malik, M. Chand, S.C. Jain, Synthesis and antimicrobial activity of some new 4-triazolylmethoxy-2H- chromen-2-one derivatives, Med. Chem. Res. 21 (11) (2012) 3750–3756, doi:10.1007/s00044-011-9881-0.
[45] R.V. Patel, J.K. Patel, P. Kumari, K.H. Chikhali, Synthesis of Novel Quinolone and Coumarin Based 1,3,4-Thiadiazolyl and 1,3,4-Oxadiazolyl -*N*-Mannich Bases as Potential Antimicrobials. Lett. Org, Chem 9 (7) (2012) 478–486, doi:10.2174/157017812802139681.
[46] Z. Jin, X. Du, Y. Xu, Y. Deng, M. Liu, Y. Zhao, B. Zhang, X. Li, L. Zhang, C. Peng, Y. Duan, J. Yu, L. Wang, K. Yang, F. Liu, R. Jiang, X. Yang, T. You, X. Liu, X. Yang, F. Bai, H. Liu, X. Liu, L.W. Guddat, W. Xu, G. Xiao, C. Qin, Z. Shi, H. Jiang, Z. Rao, H. Yang, Structure of M(pro) from SARS-CoV-2 and discovery of its inhibitors, Nature 582 (2020) 289–293, doi:10.1038/s41586-020-2223-y.
[47] Y. Gao, L. Yan, Y. Huang, F. Liu, Y. Zhao, L. Cao, T. Wang, Q. Sun, Z. Ming, L. Zhang, J. Ge, L. Zheng, Y. Zhang, H. Wang, Y. Zhu, C. Zhu, T. Hu, T. Hua, B. Zhang, X. Yang, J. Li, H. Yang, Z. Liu, W. Xu, L.W. Guddat, Q. Wang, Z. Lou, Z. Rao, Structure of the RNA-dependent RNA polymerase from COVID-19 virus, Science 368 (2020) 779–782, doi:10.1126/science.abb7498.
[48] J.C. Gordon, J.B. Myers, T. Folta, V. Shoja, L.S. Heath, A. Onufriev, a server for estimating pKas and adding missing hydrogens to macromolecules, Nucleic Acids Res 33 (Web Server issue) (2005) W368–W371, doi:10.1093/nar/gki464.
[49] G.M. Morris, R. Huey, W. Lindstrom, M.F. Sanner, R.K. Belew, D.S. Goodsell, A.J. Olson, AutoDock4 and AutoDockTools4: automated docking with selective receptor flexibility, J Comp. Chem. 30 (16) (2009) 2785–2791, doi:10.1002/jcc.21256.
[50] SZYBKI OpenEye Scientific Software: Santa Fe, 2009 NM, USA.
[51] J.M. Gasteiger, M Marsili, Iterative partial equalization of orbital electronegativity A rapid access to atomic charges, Tetrahedron 36 (22) (1980) 3219–3228.